**SUPPORTING INFORMATION FOR:**

Weyand, S., Kawajiri, K., Mortan, C. & Schebek, L. (2023.) Scheme for Generating Upscaling Scenarios of Emerging Functional Material Based Energy Technologies in Prospective LCA (UpFunMatLCA): General Methodology and Practical Implementation for the Case of Perovskite Solar Cells. *Journal of Industrial Ecology.*


**Summary**

This supporting information S1 provides more details on the development of the scheme and the data used for the practical implementation of the case study.


# 1 Introduction – Background on LCA and technology development

## 1.1 LCA description for technology developer only

LCA is a method standardized in the ISO 14040/14044 (ISO 14040 2006; ISO 14044 2006) for the evaluation of a full range of environmental impacts throughout the life cycle of products and services: It is also applied widely to technologies based on FunMat (Smith et al. 2019). The integration of LCA in the early stages of the maturation process has several advantages: LCA integrates environmental and sustainability indicators into technology development, enables the identification of unintended consequences, and gives environmental-friendly guidance before costly investments and resources are made. Technology developers can thus take actions to eliminate these consequences while supporting the prioritization of research activities (Smith et al. 2019). To this end, the following four LCA phases are applied according to the standards (ISO 14040 2006; ISO 14044 2006):

1) The **goal and scope definition (G&S)** encompasses the framework conditions such as the G&S of the LCA, the so-called functional unit as a reference unit, system boundaries, and the so-called product system. The product system represents the modeled life cycle. It is differentiated into upstream, encompassing processes from the raw material extraction to the manufacturing stage, operation, corresponding to the use phase, and downstream processes, referring to the recycling and end-of-life treatment of materials at the end of the product life cycle.

2) **Life cycle inventory (LCI)**: In this phase, extensive data collection occurs. To this end, the product system is divided into a foreground and background system. Generic or secondary data from LCA databases such as ecoinvent (ecoinvent 2020), IDEA (National Institute of Advanced Industrial Science and Technology 2018), or GaBi Databases (Sphera Solutions Inc. 2020) is usually used for the background system; the foreground system

corresponds to case study-specific data preferably from primary sources. For example, for emerging FunMat, the primary data on material inventories and processing energies are collected either from or together with technology developers during their investigations.

3) In **life cycle impact assessment (LCIA)**, the environmental impacts are quantified per impact category indicator. The considered indicators are selected depending on the G&S of the LCA study and the potential environmental impacts resulting from the assessed technology. For example, regarding climate-friendliness, LCIA focuses on energy-related impacts or other impacts involving GHG emissions rather than on impacts corresponding to materials like resource depletion or release of toxic substances during the extraction of raw materials.

4) In the **interpretation** phase as the last phase, the LCA results are processed as a basis for recommendations and decision-making, addressing uncertainty issues.

## 1.2 Systematic review on upscaling in prospective LCA

A systematic review was conducted to identify the relevant scientific works published on technology development and upscaling emerging technologies in prospective LCA. The review covered the two literature databases Web of Science and ScienceDirect using the keywords “life cycle assessment”, “LCA” combined with “upscaling”, “up-scaling”, “scale-up”, “learning” and “emerging technology” (with different spelling). As a result, we came up with 36 publications. In a first evaluation round, we checked the abstracts for the scope of the publications and excluded four publications. A second evaluation excluded publications with limited focus on a case study. Here, 19 publications were excluded. Finally, one publication was extended and in total 13 publications were assessed focusing on the topics:

- **Classification schemes of technology maturation considered**
- **Inclusiong of technology maturation**
- **Upscaling data, techniques and models**

| **Author** | **Database** | **Excluded, missing scope** | **Excluded, only case study** |
|---|---|---|---|
| Bergerson et al. (2020) | WoS or Science direct | no | no |
| Buyle et al. (2019) | WoS or Science direct | no | no |
| Cucurachi, van der Giesen, and Guinée (2018) | WoS or Science direct | no | no |
| Gavankar, Suh, and Keller (2015) | WoS or Science direct | no | no |
| Hetherington et al. (2014) | WoS or Science direct | no | no |
| Kawajiri et al. (2020) | WoS or Science direct | no | no |
| Moni et al. (2020) | WoS or Science direct | no | no |
| Thonemann and Schulte (2019) | WoS or Science direct | no | no |
| Thonemann, Schulte, and Maga (2020) | WoS or Science direct | no | no |
| Tsoy et al. (2020) | WoS or Science direct | no | no |
| van der Giesen et al. (2020) | WoS or Science direct | no | no |
| van der Hulst et al. (2020) | WoS or Science direct | no | no |
| Arvidsson et al. (2017) | Additional | no | no |

### *1.2.1 Upscaling effects: Size, learning and experience effect*

The concept of economy of scale, originating from economic analysis, is the empirical finding that manufacturing at a bigger size with a higher TRL or MRL decreases costs. In 1936, Theodore Wright described this concept mathematically by the so-called size effect as a function of the initial cost $C_0$ of the first production capacity $X_0$ to the future cost at any time $C_t$ of the future production capacity $X_t$ and the scaling factor b (Eq. 1) (Wright 1936). Eq. 1 is also known as Wright's law.

$$C_t = C_0 \left(\frac{X_t}{X_0}\right)^b \text{ (Eq. 1)}$$

The size effect in a narrower sense means the reduction of unit costs simultaneously by increasing physical dimensions such as the manufacturing size. Consequently, this effect displays any economic, technical, or other effect related merely to the size, volume, or throughput of a process or technology. Thus, factor b is derived from empirical technology data at different dimensions by using regression analysis. The rationales behind this are decreasing marginal costs by dividing overhead costs by a larger number of products and better equipment utilization.

Beyond that, Wright discovered a cost reduction due to gained experience of the employees and an associated productivity increase, the so-called learning effect. Later the Boston Consulting Group (BCG) also established the term experience effect as a collection of various learning effects (Boston Consulting Group 1968). Learning and experience effects cannot be dedicated to single changes and are usually not considered separately. Therefore, we use the term learning effect synonymously for both effects in the following. The learning effect means that technologies can be manufactured more efficiently with each increase of their cumulative production rate due to increased experience of the daily routines at the production site of mass production. This effect is modeled using the so-called experience curve concept, based on data from real manufacturing sites or market data.

## 2 Methodology of UpFunMatLCA - Scheme for Generating Upscaling Scenarios of Emerging Functional Material Based Energy Technologies in Prospective LCA

In the following, the development of the three-step scheme UpFunMatLCA are explained in more detail. The general scheme is developed using the five phases of the scenario technique of Kosow and Gassner (2008) (Table S1).

**Table S1 The connection of the generated upscaling scenarios using the three steps of UpFunMatLCA and the five phases of scenario technique of Kosow and Gassner (2008)**

| Three steps of UpFunMatLCA | Five phases of Kosow and Gassner (2008) | Explanation |
|---|---|---|
| **Aim of UpFunMatLCA** | **Phase 1: Scenario field identification** | The scenarios' purpose is to upscale an emerging FunMat from the current to a target development stage in prospective LCA. The problem of upscaling is the projection of the future process performances of emerging FunMats and modeling of life cycle inventory data based on the current stage of development. Therefore, the aim is to generate realistic scenarios that intend to represent possible development pathways of FunMats based on current technology developers' knowledge or specific decisions during technology development. These scenarios are used to model the foreground and background system and upscale the life cycle inventory data. The focus of the foreground system is not the full life cycle of FunMats but the limitation to the upstream processes, including processes from raw material extraction to manufactured FunMat. |
| **Step I: Upscaling Definition and Step II: Upscaling Leap** | **Phase 2: Identification of key factors** | The key factors or descriptors of the upscaling scenarios are the upscaling mechanisms. These are already explained in more detail in our study. To identify the key factors, we developed Step I and Step II of UpFunMatLCA. Here, first, the current and target stage is defined and results second, in a clear delimitiation of the development path and upscaling leap. Based on the upscaling leap, the relevant upscaling mechanisms are selected. |
| **Step III: Upscaling Model and Data** | **Phase 3: Analysis of the key factors** | The analysis of the key factors and the data collection process of the scenarios is implemented as upscaling modules in Step III. The upscaling module includes the upscaling method depending on the selected upscaling mechanism. |
| **Upscaling scenarios** | **Phase 4: Scenario generation** | Following the three steps of UpFunMatLCA, upscaling scenarios are generated. |
| **LCIA + interpretation of the upscaling scenarios** | **Phase 5: Scenario transfer** | The upscaling scenarios are used to model the foreground and background system and upscale LCI to assess the future possible environmental impacts of emerging FunMats in prospective LCA. Accordingly, the upscaling scenarios are transferred to the LCIA and interpretation. |

In Table S2, the template for documenting the salient characteristics of each upscaling scenario is presented.

**Table S2 Template for documenting upscaling in a prospective LCA**

| | Current stage | Target stage |
|---|---|---|
| **Step I - Upscaling Definition** | | |
| Name | | |
| General description | | |
| Generic development stage | | |
| Temporal coverage | | |
| Manufacturing dimensions | | |
| **Step II - Upscaling Leap** | | |
| Selected upscaling mechanisms | | |
| **Step III - Upscaling Data and Model** | | |
| Modeled modules | | |

## 2.1 Step I – Upscaling Definition: Definition of the technology maturity

The investigation of upscaling in terms of projection of future technology developments has since long been the interest of economics to assess impacts on production costs, unit costs of technical equipment, products, and entire businesses in the future. For this purpose, general classification schemes to describe the maturation process and the status quo of the technology development and concepts for upscaling in economics have been introduced and applied in the LCA of technology development.

In the following, we explain the development of the generic technology scale from common classification schemes of technology development and description of technology maturity.

**Table S3 Delimitation of the developed generic technology scale from common classification schemes and literature**

| **Our technology scale** | | **TRL (NASA, 2007)** | | **MRL (US DoD 2015)** | **EARTO (2014)** | **Hulst et al. (2020)** |
|---|---|---|---|---|---|---|
| Emerging | Generic conceptual | 1-2 | Basic principles and technology concept | 1-2 | Invention (TRL 1-2) | |
| | Generic lab | 3-4 | Proof-of-concept, validation in lab | 3-4 | Concept validation (TRL 3-4) | |
| | Generic pilot | 5-7 | Technology demonstration | 5-8 | Prototyping and incubation (TRL 5)<br>Pilot production and demonstration (TRL 6-7) | |
| Mature | Generic fab-early | 8-9 | System test, launch and operations | 9 | Initial market introduction (TRL 8) | Industrial early production (MPL 0-5% + 5-50%) |
| | Generic fab-mature | n.c. | | 10 | Market expansion (TRL 9) | Industrial mature production (MPL 50-100%) |

## 2.2 Step II – Upscaling Leap: Selection of upscaling mechanisms for describing the leap from current to target stage

### *2.2.1 Generic upscaling mechanism for FunMat*

#### *A) Process learning*

This mechanism subsumes innovations regarding the manufacturing processes. For a systematic distinction, we restrict process learning to the case of a given, i.e., non-changing material system, where only its specific manufacturing processes will change, i.e., the direct processing and manufacturing of FunMat. Similar to the innovative character of FunMat, these manufacturing processes may also be novel or are often only recently introduced for the respective emerging FunMat. In the terminology of LCA, these processes are attributed to the foreground system. In contrast, the background system comprehends the mining and processing processes of raw materials, the manufacturing of bulk intermediate products, and all infrastructure processes, e.g., power generation. These processes are usually long known technologies, which can generally be expected to undergo mainly incremental efficiency gains. If significant technology changes occur, they are not specific to the manufacturing of FunMat but have broader impacts on the general economy. Thus, the background system is incorporated in the upscaling mechanism C) external developments.

In LCA, the impacts of changing foreground manufacturing processes can be principally assessed via sensitivity analysis, assuming percent improvement of the processes (Glogic et al. 2019). On the one hand, the realistic setting of parameter variation requires in-depth knowledge of the specific processes for the respective FunMat and respective data, which often are not readily available. On the other hand, process changes are the most crucial aspect with impacts notably on the energy demand of emerging technologies. To account for this most crucial step, we discern three sub mechanisms:

**A-1 Size scaling:** For the mathematical implementation of this size effect into the upscaling module, we use two recently published models for size scaling (Kawajiri et al. 2020) and implement them into the size scaling module according to Eq. 2 and Eq. 3: notably for layer-based FunMat. For these types of technologies, we formulate the assumption specifically in the way that the energy demand of a process will decrease per manufactured square meter by increasing the manufacturing size from the current stage (e.g., lab samples in square centimeter range) to mass-produced goods (in $m^2$ range).

**A-2 Technological learning:** This sub mechanism reflects changes in the type of manufacturing processes from the current to target stage. These processes can, in many cases, be applied in the lab as well as large-scale manufacturing, e.g., the sputtering process (Madou 2012). However, in other cases, due to the changing requirements of mass production or automatic production lines, other manufacturing processes have to be anticipated for fab scale.

**A-3 Industrial learning:** This sub mechanism incorporates experience from daily routines at production sites of industrial manufacturing, displayed in Wright's law as well but based on production-site-specific data. If data from the industrial production site is available, the standard methods of the experience concept can be applied as shown in (Louwen et al. 2016; Bergesen and Suh 2016). However, in case of no data, the effect of industrial learning can be studied based on assumptions from general information on industrial learning of related technologies. In particular, for emerging FunMat, there is hardly any data from mass production.

***B) Material learning***

This mechanism subsumes innovations regarding the material system, including the related raw materials, and is intimately linked to the natural science-based development process of novel materials.

**B-1 Change of material system:** This sub mechanism results in a conceptual change of the entirely considered product system independently of the current stage. In LCA, for this case, no general upscaling approach can be conceived; instead, this type of change has to be mirrored by a complete change of the product system, i.e., a newly modeled LCA inventory.

**B-2 Choice of input materials:** Above the complete change of the material system, material learning may also encompass the optimization of material systems in changing single input materials. One example can be the substitution of lead by tin in PSC or the change of substrate material from glass to PET. In these cases, the original product system is kept, but respective upstream processes are substituted in LCA. However, these changes may directly influence the manufacturing processes since glass withstands higher temperatures than PET. In total, due to the wide variety of possible material changes, material learning can be characterized as a disruptive change for which the implications to another upscaling mechanism also need to be considered.

**B-3 Optimization of input materials:** Given that information on losses is available, material learning can be mirrored by sensitivity analysis. For example, findings from a study on life cycle losses of commercial PVs showed the material losses during the raw material extraction and manufacturing of two PV technologies (CdTe and CIGS) have been estimated to be between 15-37 % related to the used materials [38]. Consequently, similar projections need to be derived for FunMats used in PSC devices.

***C) External developments***

**C-1 Incremental learning of the background system:** This mechanism subsumes innovations resulting from the external progress of the background system over time. Here, integrated LCA models are developed in the literature, notably to integrate energy scenarios in LCA (Arvesen et al. 2018; Hertwich et al. 2015). By using these models, studies showed that considering the life cycle impacts of the energy transition could result in 60 % reductions of the GHG emissions of the electricity mix from 2010 to 2050 (Hertwich et al. 2015). Furthermore, for PV, temporal reductions of the primary energy consumption per energy output of even 70 % are expected from 2010 to 2050 when considering the infrastructural change of the energy system and efficiency gains of various industry sectors over time (Arvesen et al. 2018).

## 2.3 Step III - Upscaling Model and Data: Implementation of upscaling – modeling of upscaling modules for process learning

***AM-1 Technological learning module "mapping of technologies"***

No further details are necessary.

***AM-2 Size scaling module "equipment scaling"***

The empirical scaling is used when no data on the energy or power demands of the current stage is available, but only the kind of manufacturing process (e.g., sintering) and the suitable equipment (e.g., hot plate) is known. Therefore, the empirical scaling can already be applied at the conceptual scale. The empirical data usually includes the nominal power, i.e., the maximum power demand of the equipment is applied in the calculation. Therefore, the empirical scaling represents the worst-case estimation of the target power demand. In contrast, for the individual scaling, individualized consumptions from at least the lab stage are necessary to apply this model. This model is beneficial in case the actual measured power demand is far from the trend of the empirical data.

As a reference model, we define a "linear scaling" to refer to the typical way of scaling in conventional LCAs from "lab to fab" stage without considering size effects – i.e., the "non-scaling". This linear scaling is used to compare the effect of both models on the LCA results.

The graphical illustration of the two scaling models (Eq. 2-3) compared to the linear scaling is presented in Figure S1.

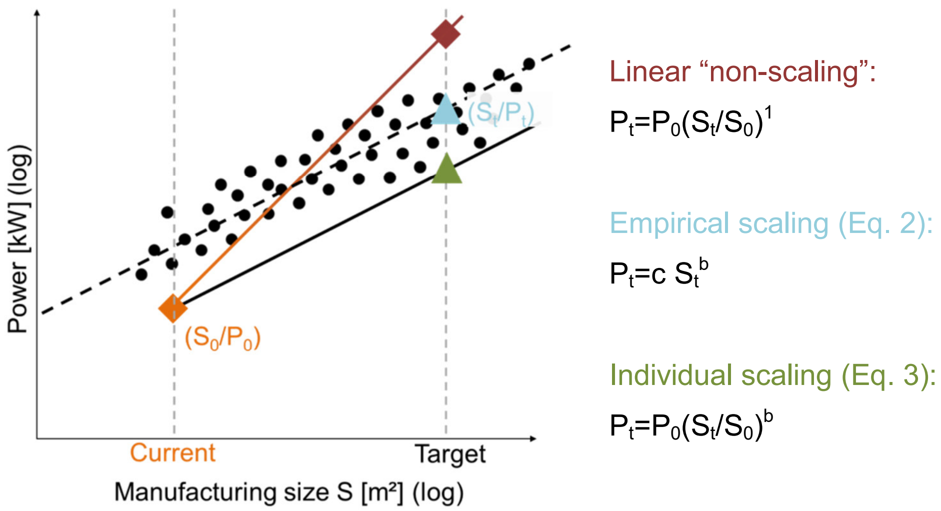


**Figure S1 Graphical illustration of the model behind the size scaling module according to (Kawajiri et al. 2020)**

***AM-3 Industrial learning module "experience of industrial manufacturing"***

No further details are necessary.

## 3 Case study: Upstream GHG Emissions of PSC from Lab to Fab

### 3.1 Case study description

#### *3.1.1 Selected PSC samples*

The PSC samples selected and assessed in this study were manufactured in lab as part of the material development of the Surface Science Group of the Technical University of Darmstadt. The interest of this material development lies in the fundamental understanding of the interplay of each layer or semiconductor band alignment (Hellmann et al. 2019; Wussler et al. 2020) to achieve high efficiencies and to find optimal layer combinations and manufacturing processes (Mortan et al. 2020; Mortan et al. 2019; Wittich et al. 2018; Dachauer et al. 2019). The selected samples are intended to represent a typical PSC material with layer materials and manufacturing methods commonly used in many research laboratories (Chen et al. 2017).

One selected sample have solar cell dimension of 32,5 $mm^2$ and a mini-module substrate dimension of 4 $cm^2$ shown in Figure S2. In addition, the detailed layer materials, thicknesses and manufacturing processes are shown in Figure S2. The detailed experimental procedure and flow chart of the manufacturing of the selected PSCs are explained in the following subsections.

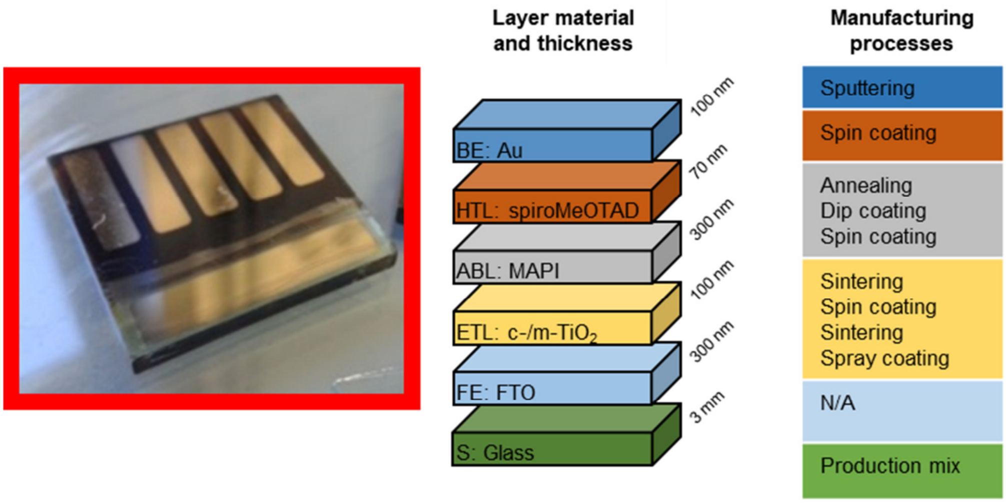


**Figure S2 Picture of one selected PSC sample and specifications on the cell architecture and manufacturing of the status quo**

The selected samples characterized electrically at the solar simulator setup, respectively through UV/Vis absorption spectroscopy, photoluminescence (PL), scanning electron microscopy (SEM), X-ray diffraction (XRD) and X-ray photoelectron spectroscopy (XPS) show a maximum power conversion efficiency of 15.6 %.

### *3.1.2 Experimental procedure*

**Front electrode with substrate (S) and front electrode (FE) (Glass coated with fluorine doped tin oxide (FTO)**: Pilkington NSG TEC15 FTO glass substrates have been used, cut as 2 cm x 2 cm squares, with a sheet resistance of 12-14 Ω/sq. and a glass thickness of 2.2 mm. The substrates are cleaned with isopropanol, soap, tap water, distilled water and blown dry with a nitrogen gun.

**Electron transport layer (ETL) (compact and mesoporous titanium dioxide (c- and m-$TiO_2$):** The c-$TiO_2$ layer is produced by spray pyrolysis on the glass/FTO substrates. 500 µL of titanium diisopropoxide bis(acetylacetonate), 75 wt. % in isopropanol (TIAA) from Merck is mixed with 18 mL reaction grade Ethanol. This solution is sprayed using oxygen carrier gas onto the glass/FTO substrates, that have been treated for 5 min. in an oxygen plasma oven and heated to 450°C for 25 min. prior to deposition. After the spraying process, the glass/FTO/c-$TiO_2$ substrates are annealed for 30 min. at 450°C in atmospheric conditions.

The m-$TiO_2$ layer is deposited by spin coating 100 µL of a 1:7 weight ratio solution of 18NR-T Titania ($TiO_2$) paste from Greatcell Solar and reaction grade ethanol onto each glass/FTO/c-$TiO_2$ substrates in atmospheric conditions. The solution is dropped on a substrate, before spinning at 83 rps (revolutions per second) for 45 s. After drying for 10 min. at 70°C, an additional sintering step takes place for 45 min. at 450°C on a hot plate, in atmospheric conditions.

**Absorber layer (ABL) ($PbI_2$- and $CH_3NH_3I$-precursor):** Prior to the deposition of the lead(II)iodide layer, the glass/FTO/c-$TiO_2$/m-$TiO_2$ substrates are treated in a UV/ozone oven for 15 min. The deposition takes place in a nitrogen ($N_2$) filled glovebox. After each substrate has been heated for 2 min. at 80°C on a hotplate, 100 µL of a 555 mg $PbI_2$ (Alfa Aesar 99.9985%, metal base) in 1 mL DMF (N,N-Dimethylformamide, Merck, 99.8%, anhydrous) solution, that has been stirred for at least half an hour at 80°C is dropped onto the hot substrates, then spun at 108 rps for 90 s. Each substrate is subsequently dried for 10 min. at 80°C.

In a nitrogen glovebox, a solution of 400 mg methylammonium iodide (MAI, Greatcell Solar) and 40 mL anhydrous 2-propanol (99.5%, Merck) is stirred at 70°C until dissolved. After reaching room temperature, the solution is added to a Petri dish containing the glass/FTO/c-$TiO_2$/m-$TiO_2$/$PbI_2$ substrates. After 2 min., each substrate is rinsed in a clean 2-propanol bath of excess MAI and immediately blown dry with a pen blower. After additional drying on a hot plate for 15 min. at 50°C in the glovebox, the substrates are annealed in a tube furnace, in atmospheric air for 20 min. at 120°C.

**Hole transport layer (HTL) (Spiro-MeOTAD):** The deposition of the spiro-MeOTAD layer takes place on the glass/FTO/c-$TiO_2$/m-$TiO_2$/MAPI substrates, in a nitrogen glovebox. 80 mg spiro-MeOTAD (Borun New Material, 99.9%) is mixed in 1 mL chlorobenzene (Merck, anhydrous, 99.8%) with 28.5 µL 4-tert-butylpyridine (Merck, 98%) and with 17.5 µL of a solution made from 260 mg Li-TFSI (bis(trifluoromethane)sulfonimide lithium salt, Merck, >99%) and 0.5 mL acetonitrile (Merck, anhydrous 99.8%). 100 µL of the resulted spiro-MeOTAD solution is dropped on a glass/FTO/c-$TiO_2$/m-$TiO_2$/MAPI substrate. After a pause of 20 s, it is spun at 23 rps for 30 s and left to dry at room temperature in the glovebox.

**Back contact with back electrode (BE) (Gold layer):** The gold (Au) layer is deposited by argon sputtering on top to the spiro-MeOTAD layer, in a Quorum Technologies Q300TD machine with 30 mA current for 120 s, using a steel mask for defining the contacts.

### *3.1.3 Detailed flow chart of the status quo*

The detailed manufacturing flow chart collected during lab visits between 2016-2018 are shown in Figure S3

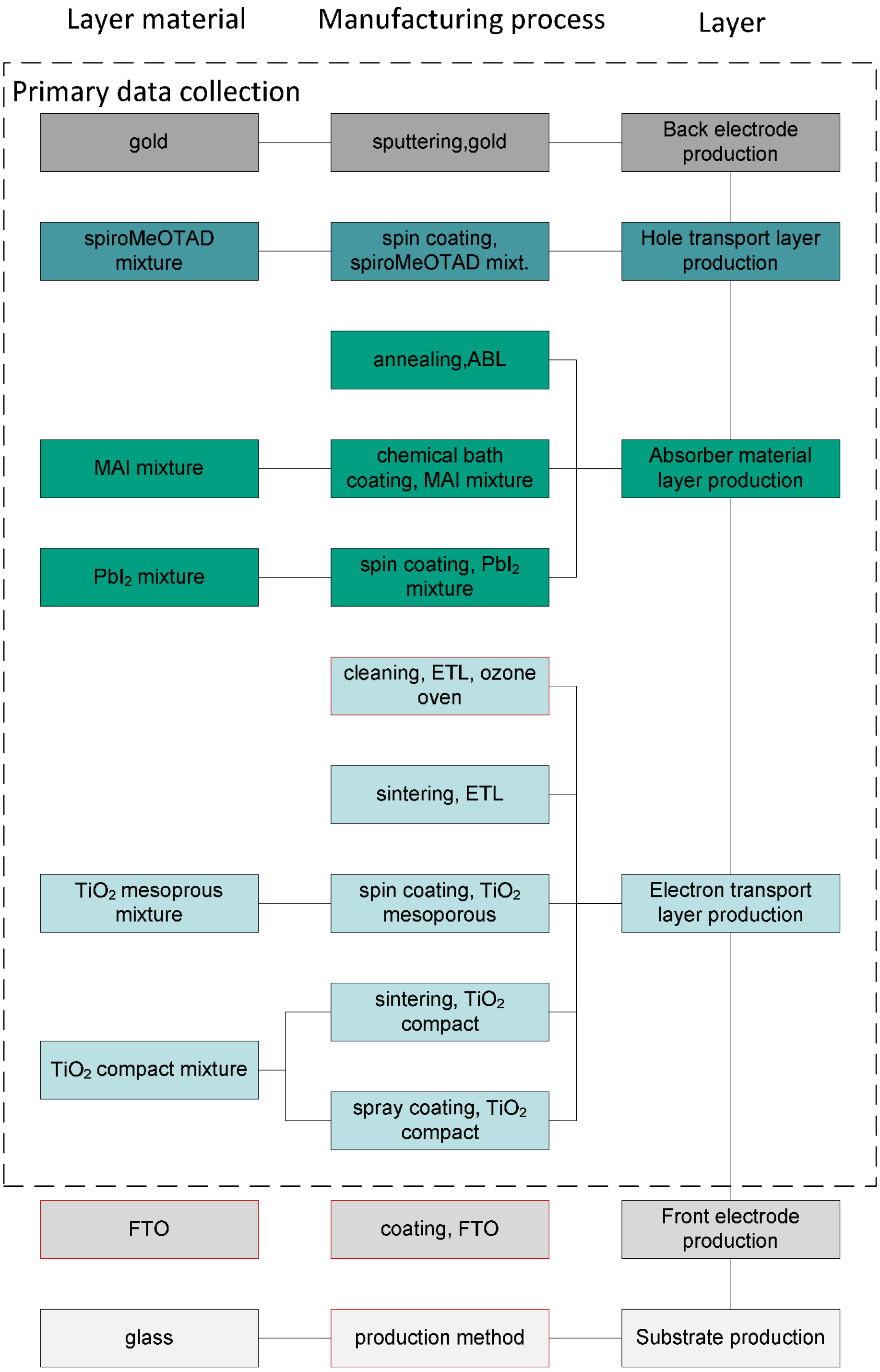


FTO: fluorine doped tin oxide, $TiO_2$: titanium dioxide, $PbI_2$: lead (II) iodide, MAI: methylammonium iodide, ETL: Electron transport layer, ABL: Absorber material or active layer

**Figure S3 Detailed process flow chart of the foreground system of the manufacturing stage**

## 3.2 Developed upscaling scenarios

### 3.2.1 *Step 1: Definition of the modelled current and target stages*

**Table S4 Generic technology scale extended by the standard cell, module, and manufacturing sizes for the definition of the technology maturity of PV case studies (adjusted and combined from (Baliozian et al. 2016; Gavankar, Suh, and Keller 2015; Fischer et al. 2020))**

| **This study** | **Generic conceptual** | **Generic lab** | **Generic pilot** | **Generic fab** | |
|---|---|---|---|---|---|
| | | | | **(early)** | **(mature)** |
| **Cell size** | - | Not classified | Not classified | 166x166 mm² | |
| **Module size** | - | >0.01 m² | 0.01-1.65 m² | 60 cells → 1.65 m²<br>72 cells →1.98 m² | |
| **Manufactured size** | - | >0.01 m² | 0.01-1.65 m² | 1-6 modules → 1.65 – 10 m² | |
| **Comparison to other literature** | | | | | |
| **TRL according to (Baliozian et al. 2016)** | 0 | 1-4 | 5-7 | 8 | 9 |
| **Cell size according to (Baliozian et al. 2016) and updated (Fischer et al. 2020)** | - | Not classified | Not classified | 125x125 or 156x156 mm²<br>166x166 or 182x182 or 210x210 mm² (2020) | |
| **Module size (Fischer et al. 2020)** | | Not classified | Not classified | 60 or 72 cells until 2030 | |

### 3.2.2 *Step 2: Selection of upscaling elements*

Upscaling from generic lab to generic fab-early or generic fab-mature results in the preselection of six mechanisms (Figure S4). The change of material system is excluded since the PSC material does not fundamentally change. We focus only on the main contributor, thus only the process learning modules are finally selected.

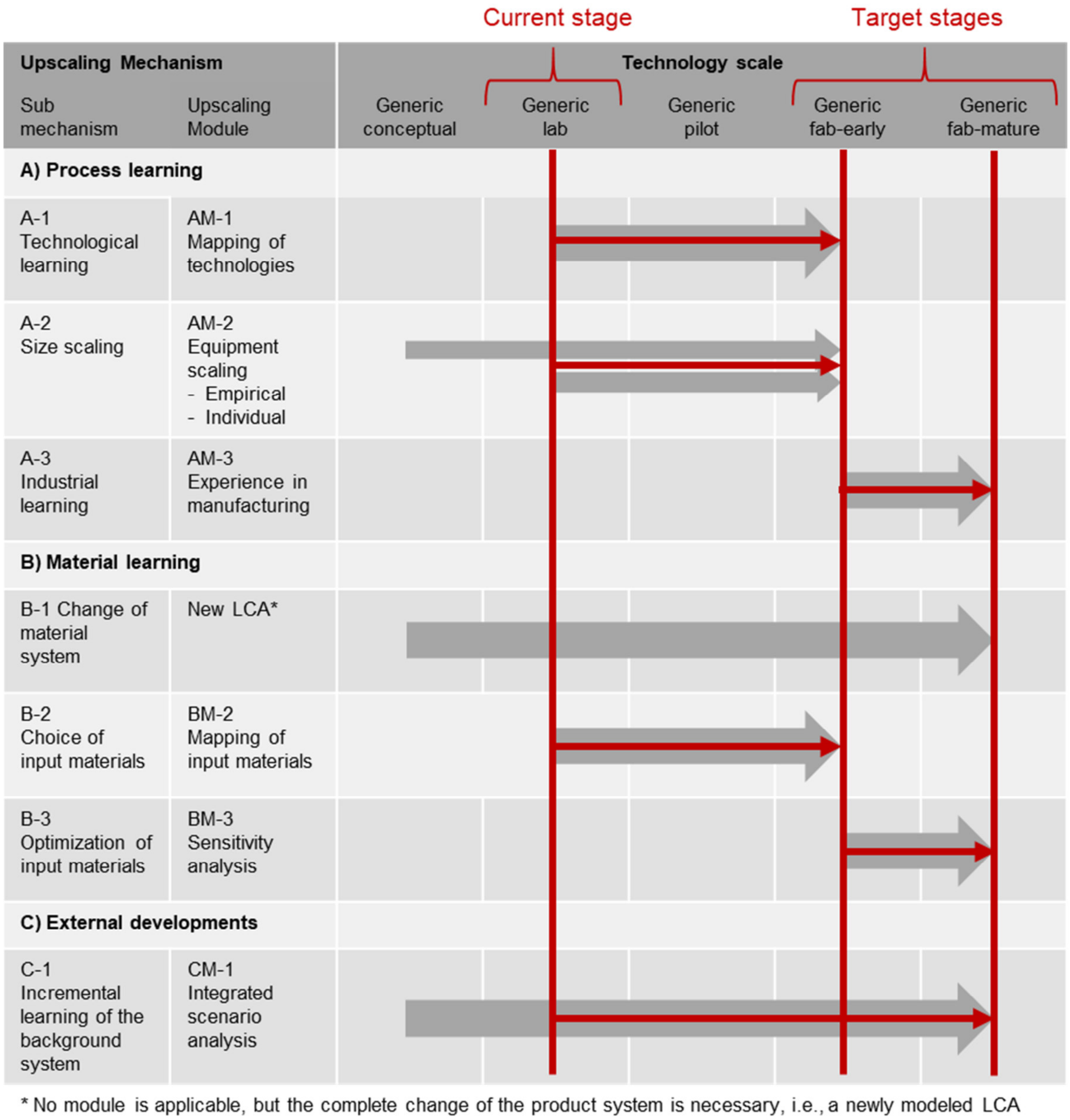


Figure S4 Selection of upscaling elements

### *3.2.3 Step 3: Extension of the LCI - Data collections of the modeled process learning upscaling modules*

***AM-1 Mapping of technologies***

The detailed description of this upscaling module AM-1 is available in the Supporting Information S2, Tabs "AM1[…]".

***AM-2 Equipment scaling – empirical and individual***

Here, only the results of the sensitivity analysis are shown in Table S5. The detailed upscaling data of this upscaling module is provided in in the Supporting Information S2, Tabs "AM2[…]"..

**Table S5 Results of the sensitivity analysis of GFabE in purple (underlying data from Table S5 are available in the Supporting Information S3, purple Tabs "Sensitivity analysis").**

| GWP 100 in kg CO2-eq / m2 | | | | | | | |
|---|---|---|---|---|---|---|---|
| sensitive indicators | | GFabE | | GFabE (linear scaling) | | GFabE (exclusion of spray coater) | |
| **perovskite solar cell production, all layers, wet chemica** | **kg CO2 eq** | **100.00%** | **200.99226** | **100.76%** | **202.5113** | **100.00%** | **200.99107** |
| *Control calculation* | | *100.00%* | *200.992281* | *100.76%* | *202.511321* | *100.00%* | *200.991091* |
| *titanium dioxide (TiO2) mixture production, for titanium dioxide (TiC* | *kg CO2 eq* | ***2.98%*** | *5.99376* | ***2.98%*** | *5.99376* | ***2.98%*** | *5.99376* |
| *titanium dioxide (TiO2) mixture production, titanium dioxide (TiO2) r* | *kg CO2 eq* | *0.12%* | *0.24227* | *0.12%* | *0.24227* | *0.12%* | *0.24227* |
| *market for gold \| gold \| Cutoff, U - GLO* | *kg CO2 eq* | *20.63%* | *41.46658* | *20.63%* | *41.46658* | *20.63%* | *41.46658* |
| *spiroMeOTAD mixture production, hole transport layer - DE* | *kg CO2 eq* | *2.47%* | *4.95939* | *2.47%* | *4.95939* | *2.47%* | *4.95939* |
| *methylammonium iodide (MAI) mixture production, active layer - DE* | *kg CO2 eq* | *1.70%* | *3.41449* | *1.70%* | *3.41449* | *1.70%* | *3.41449* |
| *lead(II) iodide mixture production, active layer - DE* | *kg CO2 eq* | *1.00%* | *2.00635* | *1.00%* | *2.00635* | *1.00%* | *2.00635* |
| *solar glass production, ecoinvent version 3.7.1 cutoff* | *kg CO2 eq* | *1.91%* | *3.83278* | *1.91%* | *3.83278* | *1.91%* | *3.83278* |
| *fluorine doped tin oxide (FTO) production, front electrode, Espinosa* | *kg CO2 eq* | *0.00%* | *1.0818E-05* | *0.00%* | *1.0818E-05* | *0.00%* | *1.0818E-05* |
| hot plate operation, during titanium dioxide compact mixture spray | kg CO2 eq | 21.34% | 42.9003 | 21.34% | 42.9003 | 21.34% | 42.9003 |
| **spray coater operation, during titanium dioxide compact mixture** | **kg CO2 eq** | **0.00%** | **0.00119** | **0.67%** | **1.35053** | **0.00%** | **0** |
| hot plate operation, during titanium dioxide compact mixture sinter | kg CO2 eq | 25.61% | 51.48036 | 25.61% | 51.48036 | 25.61% | 51.48036 |
| hot plate operation, during electron transport layer sintering, per ta | kg CO2 eq | 18.56% | 37.30461 | 18.56% | 37.30461 | 18.56% | 37.30461 |
| hot plate operation, during titanium dioxide mesoporous mixture sp | kg CO2 eq | 0.07% | 0.14922 | 0.07% | 0.14922 | 0.07% | 0.14922 |
| **spin coater operation, during titanium dioxide mesoporous mixtu** | **kg CO2 eq** | **0.00%** | **0.00436** | **0.03%** | **0.05064** | 0.00% | 0.00436 |
| vacuum pump operation, during gold sputtering, per sputtered targe | kg CO2 eq | 0.24% | 0.47596 | 0.24% | 0.47596 | 0.24% | 0.47596 |
| sputter coater operation, during gold sputtering, per target substrat | kg CO2 eq | 0.17% | 0.33722 | 0.17% | 0.33722 | 0.17% | 0.33722 |
| hot plate operation, during methylammonium iodide mixture chemi | kg CO2 eq | 0.04% | 0.07461 | 0.04% | 0.07461 | 0.04% | 0.07461 |
| hot oven operation, during annealing of active layer, per target sub | kg CO2 eq | 2.48% | 4.99422 | 2.48% | 4.99422 | 2.48% | 4.99422 |
| hot plate operation, during lead (II) iodide mixture spin coating, per | kg CO2 eq | 0.67% | 1.34297 | 0.67% | 1.34297 | 0.67% | 1.34297 |
| **spin coater operation, during lead (II) iodide mixture spin coating** | **kg CO2 eq** | **0.00%** | **0.00872** | **0.05%** | **0.10129** | 0.00% | 0.00872 |
| coating operation, during fluorine doped tin oxide coating, per targ | kg CO2 eq | 0.00% | 0 | 0.00% | 0 | 0.00% | 0 |
| **spin coater operation, during spiroMeOTAD mixture spin coating,** | **kg CO2 eq** | **0.00%** | **0.00291** | **0.02%** | **0.03376** | 0.00% | 0.00291 |
| electron transport layer production, titanium dioxide compact r | kg CO2 eq | 68.70% | 138.07606 | 68.85% | 139.4254 | 68.70% | 138.07487 |
| back electrode production, gold, wet chemical deposition, per | kg CO2 eq | 21.04% | 42.27976 | 20.88% | 42.27976 | 21.04% | 42.27976 |
| hole transport layer production, spiroMeOTAD, wet chemical | kg CO2 eq | 2.47% | 4.9623 | 2.45% | 4.9623 | 2.47% | 4.9623 |
| active layer production, CH3NH3PbI3, wet chemical depositio | kg CO2 eq | 5.89% | 11.84135 | 5.85% | 11.84135 | 5.89% | 11.84135 |
| substrate production, glass, perovskite solar cell per target sc | kg CO2 eq | 1.91% | 3.83278 | 1.89% | 3.83278 | 1.91% | 3.83278 |
| front electrode production, fluorine-doped tin oxide, wet chem | kg CO2 eq | 0.00% | 1.082E-05 | 0.00% | 1.082E-05 | 0.00% | 1.082E-05 |
| *MaE* | | *30.80%* | *61.9156308* | *30.80%* | *61.9156308* | *30.80%* | *61.9156308* |
| PEn | | 69.20% | 139.07665 | 69.95% | 140.59569 | 69.19% | 139.07546 |
| **Summe** | | **100.00%** | **200.992281** | **100.76%** | **202.511321** | **100.00%** | **200.991091** |

### *AM-3-PSC Learning rate of PSC*

No detailed upscaling data was collected.

## 3.3 Prospective upstream GHG emissions from lab to fab

The underlying data for Figure 6 are available in the Supporting Information S3.

## References


Arvesen, A., G. Luderer, M. Pehl, B. L. Bodirsky, and E. G. Hertwich. 2018. Deriving life cycle assessment coefficients for application in integrated assessment modelling. *Environmental Modelling & Software*, Vol. 99: 111–25. doi: 10.1016/j.envsoft.2017.09.010.

Arvidsson, R., A.-M. Tillman, B. A. Sandén, M. Janssen, A. Nordelöf, D. Kushnir, and S. Molander. 2017. Environmental Assessment of Emerging Technologies: Recommendations for Prospective LCA. *Journal of Industrial Ecology*, Vol. 80(7): 40. doi: 10.1111/jiec.12690.

Baliozian, P., S. Mourad, D. Morse, S. Kim, L. Friedrich, and R. Preu. 2016. Photovoltaic Development Standardizing Based on Roadmaps and Technology Readiness Levels. In

*32nd European Photovoltaic Solar Energy Conference and Exhibition: Proceedings of the international conference held in Munich, Germany, 20 June-24 June 2016*, edited by M. Topič, N. Taylor, and P. Helm, 2924–29. München, Germany, München, Germany: WIP. 6 pages / 32nd European Photovoltaic Solar Energy Conference and Exhibition; 2924-2929.

Bergerson, J. A., A. Brandt, J. Cresko, M. Carbajales-Dale, H. L. MacLean, H. S. Matthews, S. McCoy et al. 2020. Life cycle assessment of emerging technologies: Evaluation techniques at different stages of market and technical maturity. *Journal of Industrial Ecology*, Vol. 24(1): 11–25. doi: 10.1111/jiec.12954.

Bergesen, J. D. and S. Suh. 2016. A framework for technological learning in the supply chain: A case study on CdTe photovoltaics. *Applied Energy*, Vol. 169: 721–28. doi: 10.1016/j.apenergy.2016.02.013.

Boston Consulting Group. 1968. *Perspectives on Experience:* Boston Consulting Group.

Buyle, Audenaert, Billen, Boonen, and van Passel. 2019. The Future of Ex-Ante LCA? Lessons Learned and Practical Recommendations. *Sustainability*, Vol. 11(19): 5456. doi: 10.3390/su11195456.

Chen, H., F. Ye, W. Tang, J. He, M. Yin, Y. Wang, F. Xie et al. 2017. A solvent- and vacuum-free route to large-area perovskite films for efficient solar modules. *Nature*, Vol. 550(7674): 92–95. doi: 10.1038/nature23877.

Cucurachi, S., C. van der Giesen, and J. Guinée. 2018. Ex-ante LCA of Emerging Technologies. *Procedia CIRP*, Vol. 69: 463–68. doi: 10.1016/j.procir.2017.11.005.

Dachauer, R., O. Clemens, K. Lakus-Wollny, T. Mayer, and W. Jaegermann. 2019. Characterization of Methylammonium Lead Iodide Thin Films Fabricated by Exposure of Lead Iodide Layers to Methylammonium Iodide Vapor in a Closed Crucible Transformation Process. *physica status solidi (a)*, Vol. 216(11). doi: 10.1002/pssa.201800894.

ecoinvent. 2020. ecoinvent. https://www.ecoinvent.org/.

Fischer, M., M. Woodhouse, S. Herritsch, and J. Trube. 2020. International Technology Roadmap for Photovoltaic (ITRPV). 11th edition.

Gavankar, S., S. Suh, and A. A. Keller. 2015. The Role of Scale and Technology Maturity in Life Cycle Assessment of Emerging Technologies: A Case Study on Carbon Nanotubes. *Journal of Industrial Ecology*, Vol. 19(1): 51–60. doi: 10.1111/jiec.12175.

Glogic, E., A. Adán-Más, G. Sonnemann, M. d. F. Montemor, L. Guerlou-Demourgues, and S. B. Young. 2019. Life cycle assessment of emerging Ni–Co hydroxide charge storage electrodes: impact of graphene oxide and synthesis route. *RSC Adv.*, Vol. 9(33): 18853–62. doi: 10.1039/C9RA02720C.

Hellmann, T., M. Wussler, C. Das, R. Dachauer, I. El-Helaly, C. Mortan, T. Mayer, and W. Jaegermann. 2019. The difference in electronic structure of MAPI and MASI perovskites and its effect on the interface alignment to the HTMs spiro-MeOTAD and CuI, Journal of

Materials Chemistry C, 7(18), 5324-5332. Journal of Materials Chemistry C, 7(18), 5324-5332. doi: 10.1039/C8TC06332J.

Hertwich, E. G., T. Gibon, E. A. Bouman, A. Arvesen, S. Suh, G. A. Heath, J. D. Bergesen, A. Ramirez, M. I. Vega, and L. Shi. 2015. Integrated life-cycle assessment of electricity-supply scenarios confirms global environmental benefit of low-carbon technologies. *Proceedings of the National Academy of Sciences of the United States of America*, Vol. 112(20): 6277–82. doi: 10.1073/pnas.1312753111.

Hetherington, A. C., A. L. Borrion, O. G. Griffiths, and M. C. McManus. 2014. Use of LCA as a development tool within early research: Challenges and issues across different sectors. *Int J Life Cycle Assess*, Vol. 19(1): 130–43. doi: 10.1007/s11367-013-0627-8.

ISO 14040. 2006. *Environmental management – Life cycle assessment – Principles and framework*, Vol. 13.020.10, no. ISO 14040.

ISO 14044. 2006. *Environmental management - Life cycle assessment - Requirements and guidelines*, no. DIN ISO 14044.

Kawajiri, K., T. Goto, S. Sakurai, K. Hata, and K. Tahara. 2020. Development of life cycle assessment of an emerging technology at research and development stage: A case study on single-wall carbon nanotube produced by super growth method. *Journal of Cleaner Production*, Vol. 255: 120015. doi: 10.1016/j.jclepro.2020.120015.

Kosow, H. and R. Gassner. 2008. *Methods of Future and Scenario Analysis: Overview, Assessment, and Selection Criteria.* Bonn.

Louwen, A., W. G. J. H. M. van Sark, A. P. C. Faaij, and R. E. I. Schropp. 2016. Re-assessment of net energy production and greenhouse gas emissions avoidance after 40 years of photovoltaics development. *Nature communications*, Vol. 7: 13728. doi: 10.1038/ncomms13728.

Madou, M. J. 2012. *Fundamentals of microfabrication and nanotechnology. Volume II, Manufacturing techniques for microfabrication and nanotechnology.* Third edition. Boca Raton, FL: CRC Press.

Moni, S. M., R. Mahmud, K. High, and M. Carbajales-Dale. 2020. Life cycle assessment of emerging technologies: A review. *Journal of Industrial Ecology*, Vol. 24(1): 52–63. doi: 10.1111/jiec.12965.

Mortan, C., T. Hellmann, M. Buchhorn, M. d'Eril Melzi, O. Clemens, T. Mayer, and W. Jaegermann. 2020. Preparation of methylammonium lead iodide (CH 3 NH 3 PbI 3 ) thin film perovskite solar cells by chemical vapor deposition using methylamine gas (CH 3 NH 2 ) and hydrogen iodide gas, Energy Science & Engineering. Energy Science & Engineering. doi: 10.1002/ESE3.734.

Mortan, C., T. Hellmann, O. Clemens, T. Mayer, and W. Jaegermann. 2019. Preparation of Methylammonium Tin Iodide (CH 3 NH 3 SnI 3 ) Perovskite Thin Films via Flash

Evaporation, Physica status solidi (a), 216(18), 1900209. Physica status solidi (a), 216(18), 1900209. doi: 10.1002/PSSA.201900209.

National Institute of Advanced Industrial Science and Technology. 2018. IDEA v2.1.3 Database, Inventory Database for Environmental Analysis. http://idea-lca.com/.

Smith, L., T. Ibn-Mohammed, L. Koh, and I. M. Reaney. 2019. Life cycle assessment of functional materials and devices: Opportunities, challenges, and current and future trends. *J Am Ceram Soc*, Vol. 102(12): 7037–64. doi: 10.1111/jace.16712.

Sphera Solutions Inc. 2020. GaBi LCA Databases. http://www.gabi-software.com/international/databases/.

Thonemann, N. and A. Schulte. 2019. From Laboratory to Industrial Scale: A Prospective LCA for Electrochemical Reduction of CO2 to Formic Acid. *Environ. Sci. Technol.*, Vol. 53(21): 12320–29. doi: 10.1021/acs.est.9b02944.

Thonemann, N., A. Schulte, and D. Maga. 2020. How to Conduct Prospective Life Cycle Assessment for Emerging Technologies? A Systematic Review and Methodological Guidance. *Sustainability*, Vol. 12(3): 1192. doi: 10.3390/su12031192.

Tsoy, N., B. Steubing, C. van der Giesen, and J. Guinée. 2020. Upscaling methods used in ex ante life cycle assessment of emerging technologies: a review. *Int J Life Cycle Assess*, Vol. 25(9): 1680–92. doi: 10.1007/s11367-020-01796-8.

US DoD. 2015. *Manufacturing Readiness Level (MRL) Deskbook.* Washington, D.C. United States of America, Department of Defense.

van der Giesen, C., S. Cucurachi, J. Guinée, and G. J. Kramer. 2020. A critical view on the current application of LCA for new technologies and recommendations for improved practice. *Journal of Cleaner Production*(259): 120904.

van der Hulst, M. K., M. A. J. Huijbregts, N. Loon, M. Theelen, L. Kootstra, J. D. Bergesen, and M. Hauck. 2020. A systematic approach to assess the environmental impact of emerging technologies: A case study for the GHG footprint of CIGS solar photovoltaic laminate. *Journal of Industrial Ecology*, Vol. 25(7): 645. doi: 10.1111/jiec.13027.

Wittich, C., E. Mankel, O. Clemens, K. Lakus-Wollny, T. Mayer, W. Jaegermann, and H.-J. Kleebe. 2018. Structural and compositional characteristics of vacuum deposited methylammonium lead halide perovskite layers in dependence on background pressure and substrate temperature, Thin Solid Films, 650, 51-57. Thin Solid Films, 650, 51-57. doi: 10.1016/J.TSF.2018.02.004.

Wright, T. P. 1936. Factors Affecting the Cost of Airplanes. *Journal of the Aeronautical Sciences*, Vol. 3(4): 122–28. doi: 10.2514/8.155.

Wussler, M., T. Mayer, C. Das, E. Mankel, T. Hellmann, C. Prabowo, I. Zimmermann, M. K. Nazeeruddin, and W. Jaegermann. 2020. Tapered Cross-Section Photoelectron Spectroscopy of State-of-the-Art Mixed Ion Perovskite Solar Cells: Band Bending Profile in

the Dark, Photopotential Profile Under Open Circuit Illumination, and Band Diagram, Advanced Functional Materials, 30(27), 1910679. Advanced Functional Materials, 30(27), 1910679. doi: 10.1002/ADFM.201910679.